Contribution from the Chemistry Department,
University of Virginia, Charlottesville, Virginia 22901

Laser-Raman and Emission Spectra of the Dibromide Molecular Anion in the $M^+Br_2^-$ Species

CHARLES A. WIGHT, BRUCE S. AULT, and LESTER ANDREWS*

Received February 20, 1976 AIC60141J

The argon matrix reaction product $M^+Br_2^-$ has been studied using laser excitation of alkali metal–bromine samples. The intraionic $(Br \leftrightarrow Br)^-$ stretching mode has been observed in the 149–160-cm^{-1} range for each of the alkali metal analogues, except $Na^+Br_2^-$ where the interionic $Na^+ \leftrightarrow Br_2^-$ stretching mode strongly interacts with the intraionic mode resulting in 194- and 115-cm^{-1} values, respectively. Emission spectra for $M^+Br_2^-$, $M^+Br_3^-$, and Br_2 have been correlated with optical absorptions, and an intensity dependence for Raman spectra of Br_2^- on the absorption coefficient at the laser exciting wavelength has been noted.

Introduction

This work, the fourth in a series studying charge-transfer reactions between alkali metal atoms and halogen molecules in argon matrices, was prompted by laser-Raman investigations of $M^+F_2^-$, $M^+Cl_2^-$, and $M^+I_2^-$ [1-3] and an optical absorption study of all of the $M^+X_2^-$ dihalide species.[4] The matrix-isolated $M^+Br_2^-$ ion pair exhibited a strong $\sigma \rightarrow \sigma^*$ absorption near 365 nm and a weak $\pi^* \rightarrow \sigma^*$ band near 660 nm. These absorptions had a major effect on laser-excitation studies of alkali metal–bromine matrix reactions, which are detailed here.

Experimental Section

The instruments and experimental techniques have been described previously in papers from this laboratory.[5,6] Bromine (Mallinckrodt) was purified by outgassing the solid under vacuum at liquid nitrogen temperature. Argon matrix gas (Air Products) was used without further purification; $Ar:Br_2$ ratios varied from 250:1 to 700:1. Atomic beams of Li, Na, and K were obtained after outgassing the metals in a Knudsen cell under vacuum behind a sliding door and heating until the vapor pressure of the metal was approximately 1 μ. Rubidium and cesium were evaporated from the Knudsen cell by reacting Li with RbCl and CsCl.[7]

Samples were deposited onto a 12 K tilted copper wedge at a rate of 3–5 mmol/h and monitored visually for approximately 3 h and irradiated with 476.5-, 488.0-, and 514.5-nm light from an argon ion laser and 568.2- and 647.1-nm light from a krypton ion laser (Coherent Radiation). Laser power varied from 30 to 100 mW at the sample. Raman spectra were recorded using 500-μ slits on a Spex Ramalog with a FW 130 photomultiplier tube (ITT). Dielectric filters were used to eliminate laser plasma lines from the spectra; Raman bands were calibrated with respect to plasma lines by replacing the dielectric filters with a neutral density filter.

Results

Laser excitation studies of alkali metal–bromine matrix reactions will be described, followed by additional studies of the lithium– and cesium–iodine reactions.

Bromine. Argon–bromine samples ($Ar:Br_2$ = 300:1 and 400:1) were studied in two experiments without alkali metal atoms. No Raman bands were observed using 647.1-nm excitation and the 568.2-nm line revealed a weak signal near 295 cm^{-1}. The 488.0- and 476.5-nm excitation produced two signals shifted 275 and 295 cm^{-1} from the exciting line. Previous Raman work on bromine in solid argon revealed a Raman band at 295 cm^{-1} for aggregated bromine in solid argon.[8] The 270-cm^{-1} signal appeared strongly using 476.5-nm excitation; it is probably due to IBr produced by reaction of Br_2 with residual I_2 in the vacuum system.[9]

A thorough study of alkali metal–bromine matrix reactions was conducted in 28 separate experiments. This was the most difficult of the halogen studies since the product signal was weakest and a minimum of three experiments was required with each metal to optimize reagent concentrations.

Lithium isotopic experiments were performed with $Ar:Br_2$ = 300:1, 500:1, and 700:1 samples. The red and yellow laser lines produced Raman signals at 149 and 310 ± 3 cm^{-1} which are shown in the top trace of Figure 1. Blue laser excitation gave a weak 149-cm^{-1} signal with stronger 270-cm^{-1} (IBr impurity) and 295-cm^{-1} (bromine aggregate) bands.

When an atomic beam of sodium was deposited with $Ar-Br_2$ samples using several concentrations, red laser excitation revealed two Raman signals shifted 115 and 194 ± 2 cm^{-1} from the exciting line, which are shown in Figure 1(b). The 115-cm^{-1} signal was more intense by a factor of 2. Yellow excitation produced no bands, while green and blue lines gave the 270-cm^{-1} impurity and 295-cm^{-1} bromine bands.

Five experiments with potassium and bromine yielded a 160 ± 2 cm^{-1} signal with 647.1-nm excitation, Figure 1(c). Yellow and green laser lines gave no Raman signal; however, 488.0-nm excitation gave the 160 ± 2 cm^{-1} signal and the 270- and 295-cm^{-1} bands.

In rubidium experiments, red, yellow, and green laser excitation produced a weak Raman signal at 159 ± 3 cm^{-1} and a larger 310 ± 3 cm^{-1} band, which are illustrated in Figure 1(d). Blue excitation revealed the 159 ± 3 cm^{-1} signal and the 270- and 295-cm^{-1} bands.

Cesium experiments with bromine irradiated with 647.1-nm light produced signals at 157 and 311 ± 3 cm^{-1} which are shown in Figure 1(e). Spectra using different exciting lines on the $Cs-Br_2$ sample are contrasted in Figure 2. The 157 ± 3 cm^{-1} signal was stronger with red-yellow and blue excitation than with green excitation, while the signal near 300 cm^{-1} changes from 311 cm^{-1} with red to 295 cm^{-1} with blue excitation.

When exploring the far-red shifted regions in the alkali metal–bromine systems, several new unstructured emissions were observed. Figure 3 is representative of the emission spectra recorded for all alkali metal–bromine reactions using 488.0-, 568.2-, and 647.1-nm excitation; absorption spectra for Cs + Br_2 and absorption and emission spectra from the CsBr + Br_2 system[4,10] are shown for comparison. Blue 488.0-nm excitation produced a strong emission at 600 ± 10 nm in the alkali metal–bromine systems along with an intense pattern of 300 cm^{-1} spaced triplets due to isolated Br_2 emission[6] which reached a maximum at 800 nm. A weak broad emission at 750 ± 10 nm was observed in experiments using Rb and Cs. Yellow 568.2-nm illumination yielded a weak 600-nm band and structured Br_2 emissions superposed on a strong 750 ± 10 nm emission. Red 647.1-nm excitation produced strong emissions at 740 ± 10 nm as shown in Figure 3 for the K + Br_2 reaction. The 647.1-nm excited emission near 740 nm were 2–3 orders of magnitude more intense than the Raman signals near 150 cm^{-1} in these systems. Throughout these studies, the 740–750-nm emissions were more intense with red than yellow laser excitation. A strong 685-nm emission was observed in some, but not all, of the yellow excitation studies and a shoulder near 680 nm appeared on some of the red pumped emissions. The 685-nm emission

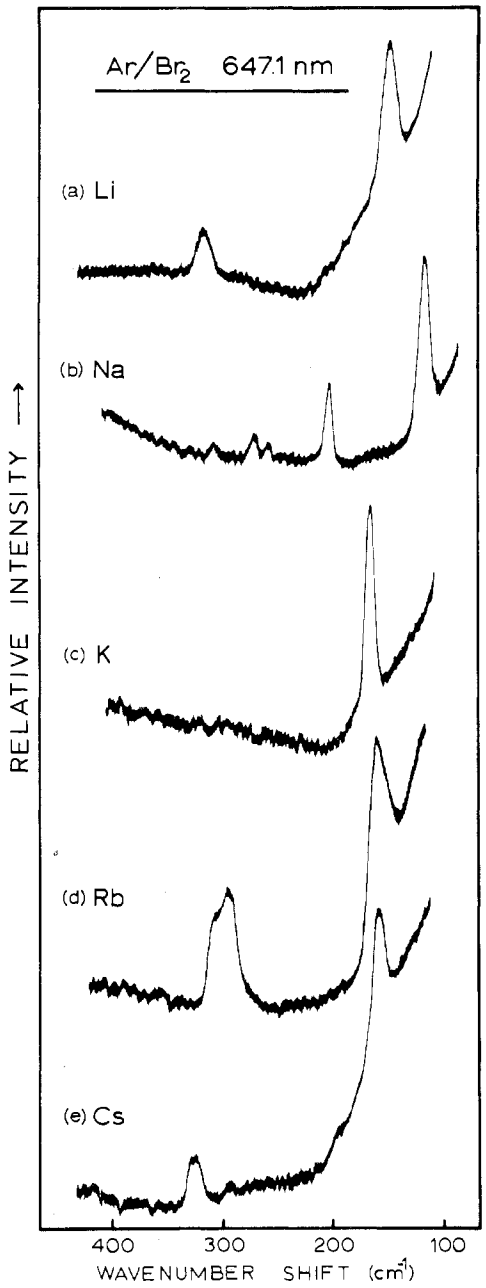

Figure 1. Raman spectra for alkali metal–bromine matrix reaction products using 100 mW of 647.1-nm laser excitation at the sample; $Ar:Br_2$ = 300:1 to 500:1; scan speed 20 cm^{-1} min; 500-μ slit width; block temperature 12 K.

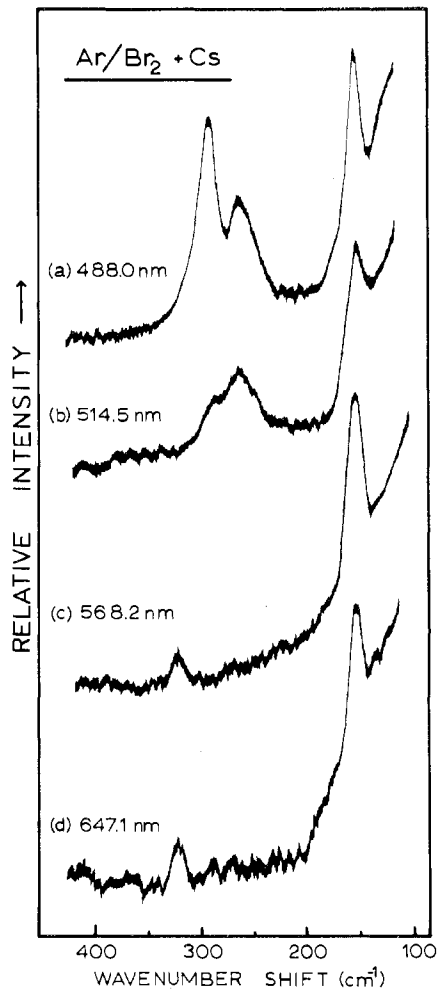

Figure 2. Raman spectra using different laser exciting lines for cesium–bromine matrix reaction products; $Ar:Br_2$ = 500:1; laser power varied between 100 and 300 mW at the sample.

Table I. Vibrational Fundamentals (cm^{-1}) for the Intraionic $(X \longleftrightarrow X)^-$ Stretching Mode of the $M^+X_2^-$ Species

	X_2^-			
M^+	F_2^- [a]	Cl_2^- [b]	Br_2^- [c]	I_2^- [d]
Li^+	452	246	149	115
Na^+	475	225	115	114
K^+	464	264	160	113
Rb^+	462	260	159	116
Cs^+	459	259	157	115

[a] Reference 1; 488.0-nm excitation, error limits ±1 cm^{-1}. [b] Reference 2; 488.0-nm excitation, error limits ±1 cm^{-1}. [c] This work; 647.1-nm excitation, error limits ±3 cm^{-1}. [d] Reference 3; 647.1-nm excitation, error limits ±3 cm^{-1}.

intensity varied over a factor of 30 with changes in alkali metal concentration relative to the 740-nm emission intensity. This suggests that the 685-nm emission is due to an aggregate species involving excess alkali atoms, and it is not of interest as a primary reaction product.

Iodine. Two additional experiments were performed with the cesium–iodine system using $Ar:I_2$ = 500:1 and 1000:1 samples and less cesium than the previous study. With 647.1-nm excitation, a strong 118 ± 3 cm^{-1} fundamental with 235, 350, and 465 ± 3 cm^{-1} overtones and a strong 737-nm emission were observed. These Raman bands are sharper and less intense than those observed in the earlier experiments which employed a greater cesium concentration. Using 488.0-nm excitation, the 118 ± 3 cm^{-1} fundamental and a weak, broad I_2 emission at 580 nm were observed.

Lithium experiments were run with $Ar:I_2$ = 1000:1 and 1200:1 samples. Using 647.1-nm excitation, a strong 114 ± 3 cm^{-1} fundamental with 226- and 338-cm^{-1} overtones and a strong 743-nm emission were recorded. Similar strong emissions were observed in the previous[3] alkali metal–iodine experiments using red laser excitation.

Discussion

Raman spectra of reaction products in the alkali metal–bromine system were the weakest observed for the halogen reactions. These Raman signals and several strong emission bands are discussed below.

Raman Spectra. The Raman signals observed in the present work are contrasted in Table I with $(X \leftrightarrow X)^-$ fundamentals from the previous studies.[1-3] The $M^+Br_2^-$ species is an intermediate in reaction 1 which is trapped by the argon matrix.

$$M + Br_2 \rightarrow M^+Br_2^- \rightarrow MBr + Br \quad (1)$$

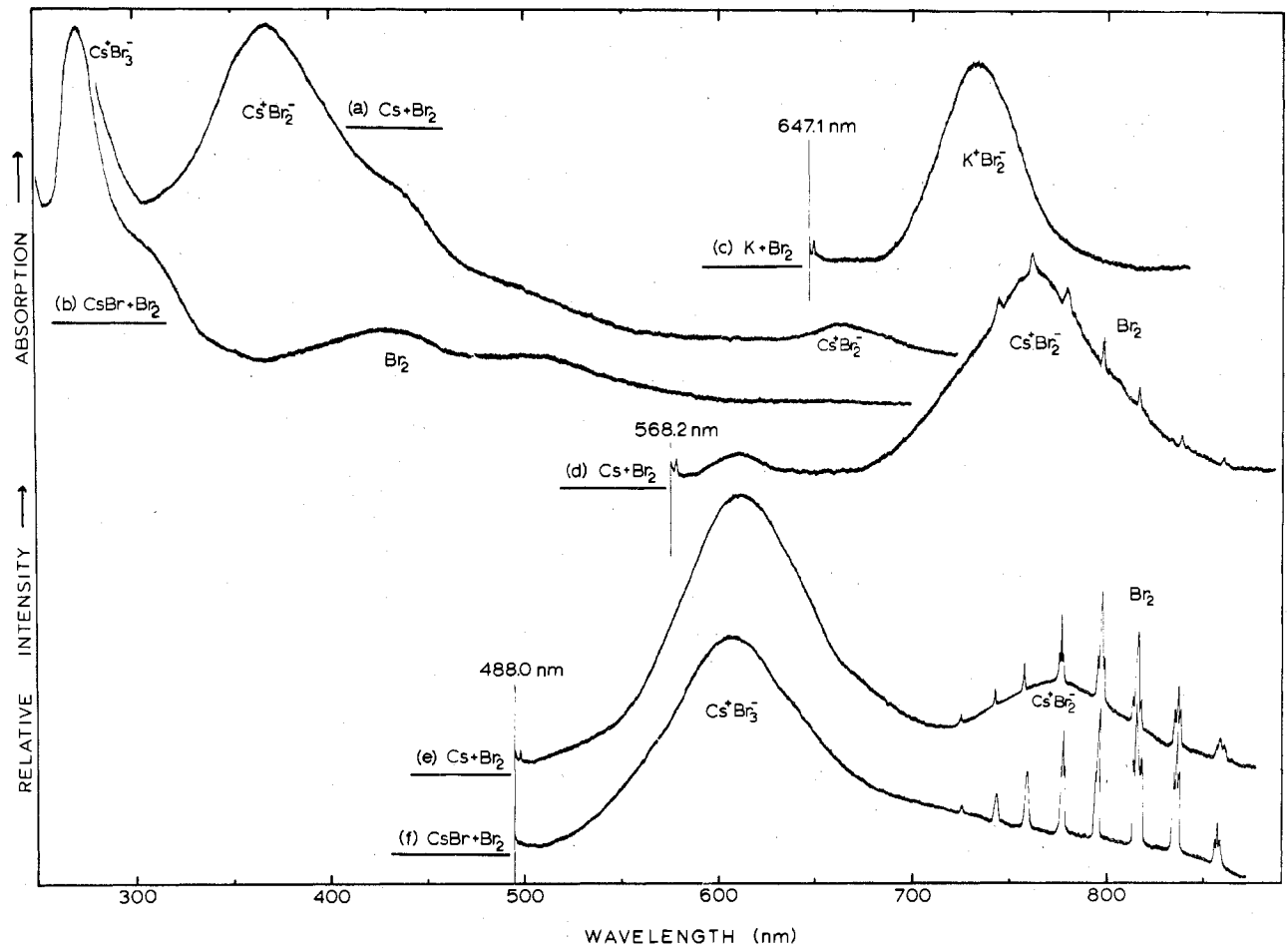

Figure 3. Optical spectra for alkali metal–bromine matrix reaction products. Absorption spectra are shown for (a) Cs codeposited with $Ar:Br_2 = 200:1$ and (b) CsBr in the salt reaction with bromine, $Ar:Br_2 = 200:1$. The emission spectrum (c) is representative of alkali metal experiments with 647.1-nm laser excitation, which shows potassium and $Ar:Br_2 = 500:1$ scanned at 200 cm^{-1}/min. Traces (d) and (e) show the emission spectra using yellow and blue laser excitation for experiments codepositing Cs and $Ar:Br_2 = 300:1$. The 488.0-nm laser excitation of matrix samples with CsBr and $Ar:Br_2 = 300:1$ yielded the emission spectrum shown in trace (f).

The red-excited Raman signals are assigned to ν_1, the $(Br \leftrightarrow Br)^-$ intraionic mode in the $M^+Br_2^-$ species owing to the presence of a weak red absorption band near 660 nm for this species which probably produces resonance intensity enhancement of the signal. The weaker band near 310 cm^{-1} in Li, K, Rb, and Cs experiments could be a first overtone, but isolated Br_2 produces a scattered signal near 315 cm^{-1},[5] and even though no 310-cm^{-1} signal was detected in the argon–bromine experiments without alkali metal, isolated Br_2 is the more likely origin of the 310-cm^{-1} signal. Furthermore, the 149 ± 3 cm^{-1} fundamental in lithium–bromine experiments should not have a 310-cm^{-1} overtone.

The secondary product species, $M^+Br_3^-$, reaction 2, is

$$MBr + Br_2 \rightarrow M^+Br_3^- \quad (2)$$

produced in decreasing yields with the heavier halogens.[4] Even though Br_3^- has a ν_1 fundamental near 160 cm^{-1},[10] this species has no allowed red absorption[11] and it is a highly unlikely origin for the red-scattered Raman signals.

Blue excitation produced the same fundamentals for the Li, K, Rb, and Cs species which are also probably due to $M^+Br_2^-$ since the strong optical band of $M^+Br_2^-$ absorbs nearest the blue at 365 nm, in contrast to $M^+Br_3^-$, which has a strong 268-nm absorption.[4]

The sodium reaction product species did not reveal Raman bands between 149 and 160 cm^{-1}, the position of the $(Br \leftrightarrow Br)^-$ mode with the other $M^+Br_2^-$ species. Instead, Raman bands were observed at 115 and 194 cm^{-1} (using 647.1-nm excitation), which have a 155-cm^{-1} midpoint. The ν_2 ($M^+ \leftrightarrow Br_2^-$) interionic mode is predicted to fall below the 229- and 202-cm^{-1} stretching modes[12] of $(Na^+Br^-)_2$ by the following argument. In lithium–chlorine studies, four infrared absorptions were observed[2] in the lithium–chloride dimer stretching region for each lithium isotope; the two middle bands at 489 and 481 cm^{-1} are due to $(^7Li^+Cl^-)_2$; the upper 518-cm^{-1} band, incorrectly assigned[2] to $Li^+Cl_2^-$, is in fact due to ^7LiCl complexed to water;[13] the lower 470-cm^{-1} band is assigned to the interionic mode in $^7Li^+Cl_2^-$, since it was absent in salt studies but present in lithium–chlorine reaction samples. In addition, $(Na^+Cl^-)_2$ exhibits strong infrared bands[12] at 272 and 227 cm^{-1}, and we now believe that the 275-cm^{-1} Raman band in sodium–chlorine studies[2] is due in part to the interionic mode in $Na^+Cl_2^-$, which mixes with the $(Cl \leftrightarrow Cl)^-$ mode at 225 cm^{-1} and is responsible for its displacement to lower frequencies relative to the interionic modes for the other $M^+Cl_2^-$ species.[2] Accordingly, the interionic $Na^+ \leftrightarrow Br_2^-$ mode is estimated to fall near 200 cm^{-1} by extending the $(^7Li^+Cl^-)_2$ and $(Na^+Cl^-)_2$ frequencies to the sodium bromide system. Therefore, the two Raman bands at 194 and 115 cm^{-1} are best assigned as the interionic and intraionic modes of $Na^+Br_2^-$, respectively, which interact strongly and separate due to their almost accidental degeneracy. Owing to this strong interaction, the interionic mode is observed in the Raman spectrum with approximately half the intensity of the intraionic mode, even though interionic modes normally have very low Raman intensity.

The general positions of the $(Br \leftrightarrow Br)^-$ modes for the other $M^+Br_2^-$ species reflect weak interactions with their respective $M^+ \leftrightarrow Br_2^-$ modes. The ν_2 mode for $Li^+Br_2^-$ is expected around

400 cm^{-1} which produces a weak interaction with ν_1 and the slightly lower 149-cm^{-1} position. The ν_2 mode for the $K^+Br_2^-$ is expected around 120 cm^{-1} and interaction forces ν_1 to higher frequencies. With increasing alkali metal atom mass, the ν_2 position falls to lower frequencies, the interaction between ν_1 and ν_2 decreases, and, accordingly, the ν_1 position decreases slightly. The dihalide vibrational modes as a function of M^+ are listed in Table I.

The general trend in Raman intensities with exciting wavelength follows the absorption spectrum for $M^+Br_2^-$; stronger Raman signals were observed with red-yellow and blue excitation, near regions of absorption.[4] The strong $\sigma \rightarrow \sigma^*$ transitions of $Cs^+Cl_2^-$, $Cs^+Br_2^-$, and $Cs^+I_2^-$ appeared at 344, 365, and 382 nm, respectively, in absorption; however, the greatest resonance Raman intensity enhancement with blue laser lines was found with $Cs^+Cl_2^-$. In the red region, the $\pi^* \rightarrow \sigma^*$ transitions of $Cs^+Br_2^-$ and $Cs^+I_2^-$ gave absorptions at 660 and 686 nm, respectively, and the latter was clearly more intense than the former.[4] Owing to the greater red absorption coefficient for I_2^- as compared to Br_2^-, the 647.1-nm excited Raman intensity of the I_2^- species was strongly resonance enhanced for $M^+I_2^-$ whereas the present Br_2^- Raman spectrum probably sustained a small amount of resonance intensity enhancement.

Emission Spectra. Turning to the broad bands observed in the emission region for the alkali metal–bromine reactions, the dominant features common to all of the systems studied were the strong emissions centered near 600 and 740 nm. Experiments using alkali bromide and bromine reagents revealed the 600-nm feature, but not the 740-nm emission.[10] Since the absorption spectrum of the CsBr + Br_2 reaction system revealed a strong 268-nm band for $Cs^+Br_3^-$,[4] which is also illustrated in Figure 3, the 600-nm emission is assigned to $Cs^+Br_3^-$, which is a secondary product in the matrix reaction of cesium and bromine. The strong 740-nm emission is unique to the alkali metal–bromine systems, and it is attributed to $M^+Br_2^-$.

The electronic transitions responsible for these emissions can be identified from the absorption spectra. The dibromide anion has a weak red absorption at 660 nm and the 647.1-nm laser line is strongly absorbed which gives the prominent 740-nm emission. The 568.2-nm laser line picks up the blue tail of the red Br_2^- absorption band and produces the 740-nm emission, although with less intensity than the red laser line. Since the diiodide anion exhibits a strong red absorption near 680 nm, the observation of a similar 740-nm emission for $M^+I_2^-$ supports the assignment of the 740-nm emission to $M^+Br_2^-$. The 0–0 band for the $\pi^* \rightarrow \sigma^*$ transition of Br_2^- in the $M^+Br_2^-$ species can be predicted midway between the emission and absorption bands at approximately 700 nm.

The absorption maximum of Br_2 at 415 nm[4] is well above the dissociation limit at 511 nm[14] and the absorption tails out through the visible region; the Br_2 emission peaks in the near-infrared region at 800 nm.[5] The strong 268-nm absorption of $Cs^+Br_3^-$ also tails, with diminishing absorption coefficient, out into the visible region. Hence, absorption of the blue laser lines and the present emissions can be associated with the transition for $Cs^+Br_3^-$ which peaks at 268 nm.

Conclusions

Raman spectra were observed for the matrix reaction product $M^+Br_2^-$ for each alkali metal species. $(Br \leftrightarrow Br)^-$ stretching fundamentals were found in the 149–160 cm^{-1} range except for $Na^+Br_2^-$ where interaction with the $Na^+ \leftrightarrow Br_2^-$ mode forced the $(Br \leftrightarrow Br)^-$ mode down to 115 cm^{-1}. The observed Br_2^- Raman intensities using different exciting lines generally correlated with the absorption spectrum. Strong emission bands were observed for $M^+Br_2^-$ and $M^+Br_3^-$ at 740 and 600 nm, respectively.

Acknowledgment. The authors gratefully acknowledge support of this research by the National Science Foundation under Grant GP-38420X and an Alfred P. Sloan fellowship for L.A.

Registry No. $Li^+Br_2^-$, 59141-10-5; $Na^+Br_2^-$, 59141-11-6; $K^+Br_2^-$, 59141-09-2; $Rb^+Br_2^-$, 59125-55-2; $Cs^+Br_2^-$, 59141-08-1.

References and Notes

(1) W. F. Howard, Jr., and L. Andrews, *J. Am. Chem. Soc.*, **95**, 3045 (1973); *Inorg. Chem.*, **14**, 409 (1975).
(2) W. F. Howard, Jr., and L. Andrews, *J. Am. Chem. Soc.*, **95**, 2056 (1973); *Inorg. Chem.*, **14**, 767 (1975).
(3) W. F. Howard, Jr., and L. Andrews, *J. Am. Chem. Soc.*, **97**, 2956 (1975).
(4) L. Andrews, *J. Am. Chem. Soc.*, **98**, 2147, 2152 (1976).
(5) B. S. Ault, W. F. Howard, Jr., and L. Andrews, *J. Mol. Spectrosc.*, **55**, 217 (1975).
(6) D. A. Hatzenbuhler and L. Andrews, *J. Chem. Phys.*, **56**, 3398 (1972).
(7) R. C. Spiker, Jr., and L. Andrews, *J. Chem. Phys.*, **58**, 713 (1973).
(8) W. F. Howard, Jr., and L. Andrews, *J. Raman Spectrosc.*, **2**, 447 (1974).
(9) C. A. Wight, B. S. Ault, and L. Andrews, *J. Mol. Spectrosc.*, **56**, 239 (1975).
(10) B. S. Ault and L. Andrews, *J. Chem. Phys.*, in press.
(11) W. Gabes and D. J. Stufkens, *Spectrochim. Acta, Part A*, **30**, 1835 (1974).
(12) B. S. Ault and L. Andrews, *J. Chem. Phys.*, **64**, 1986 (1976).
(13) B. S. Ault and G. C. Pimentel, *J. Phys. Chem.*, **79**, 621 (1975).
(14) G. Herzberg, "Spectra of Diatomic Molecules", 2d ed, Van Nostrand, Princeton, N.J., 1950.

Contribution from the Chemistry Department, University of Tasmania, Hobart, Tasmania 7001 Australia

Electronic Spectrum of the $Cu(H_2O)_6^{2+}$ Ion

M. A. HITCHMAN* and T. D. WAITE

Received October 28, 1975 AIC50775A

The electronic spectra of the compounds $Cat_2Cu(SO_4)_2 \cdot 6H_2O$ [Cat = K, Rb, Tl, NH_4] and $K_2Cu(ZrF_6)_2 \cdot 6H_2O$ and their deuterated analogues have been recorded, either as single crystals or as mulls, in the range 5000–25 000 cm^{-1}. In each case, the spectrum of the $Cu(H_2O)_6^{2+}$ ion consists of three peaks, centered at ~7500, ~10 000, and ~12 000 cm^{-1}, except for the ammonium salt, for which all four "d–d" transitions were resolved. The spectra have been assigned from the polarization properties of the peaks. The orbital energies are discussed in terms of the geometry of the $Cu(H_2O)_6^{2+}$ ion and the angular overlap simple molecular orbital bonding scheme is used to derive σ- and π-bonding parameters for the water molecule toward copper(II).

Introduction

Probably because of their comparative simplicity, aquo complexes have often formed the basis of theoretical and practical investigations into the electronic structure of transition metal complexes.[1-6] The copper Tutton salts, of general formula $(Cat)_2Cu(SO_4)_2 \cdot 6H_2O$ (Cat = cation),